

# Circulation

JOURNAL OF THE AMERICAN HEART ASSOCIATION



## **Early Contrast-Enhanced MRI Predicts Late Functional Recovery After Reperfused Myocardial Infarction**

Walter J. Rogers, Jr, Christopher M. Kramer, Gennady Geskin, Yong-Lin Hu, Therese M. Theobald, Diane A. Vido, Susan Petruolo and Nathaniel Reichek

*Circulation* 1999;99:744-750

Circulation is published by the American Heart Association, 7272 Greenville Avenue, Dallas, TX 75214  
Copyright © 1999 American Heart Association. All rights reserved. Print ISSN: 0009-7322. Online  
ISSN: 1524-4539

The online version of this article, along with updated information and services, is located on the World Wide Web at:

<http://circ.ahajournals.org/cgi/content/full/99/6/744>

Subscriptions: Information about subscribing to *Circulation* is online at  
<http://circ.ahajournals.org/subscriptions/>

Permissions: Permissions & Rights Desk, Lippincott Williams & Wilkins, a division of Wolters Kluwer Health, 351 West Camden Street, Baltimore, MD 21202-2436. Phone: 410-528-4050. Fax: 410-528-8550. E-mail:  
[journalpermissions@lww.com](mailto:journalpermissions@lww.com)

Reprints: Information about reprints can be found online at  
<http://www.lww.com/reprints>

# Early Contrast-Enhanced MRI Predicts Late Functional Recovery After Reperfused Myocardial Infarction

Walter J. Rogers, Jr, MS; Christopher M. Kramer, MD; Gennady Geskin, MD; Yong-Lin Hu, PhD; Therese M. Theobald, RDCS; Diane A. Vido, MS; Susan Petruolo, RN; Nathaniel Reichek, MD

**Background**—We have observed 3 abnormal patterns on contrast-enhanced MRI early after reperfused myocardial infarction (MI): (1) absence of normal first-pass signal enhancement (HYPO), (2) normal first pass signal followed by hyperenhanced signal on delayed images (HYPER), or (3) both absence of normal first-pass enhancement and delayed hyperenhancement (COMB). This study examines the association between these patterns in the first week after MI and late recovery of myocardial contractile function by use of magnetic resonance myocardial tissue tagging.

**Methods and Results**—Seventeen patients (14 men) with a mean age of  $53 \pm 12$  years were studied after a reperfused first MI. Contrast-enhanced images were acquired immediately after bolus administration of gadolinium and  $7 \pm 2$  minutes later. Tagged images were acquired at weeks 1 and 7. Circumferential segment shortening (%S) was measured in regions displaying HYPER, COMB, or HYPO contrast patterns and in remote regions (REMOTE) at weeks 1 and 7. At week 1, %S was depressed in HYPER, COMB, and HYPO ( $9 \pm 8\%$ ,  $7 \pm 6\%$ , and  $5 \pm 4\%$ , respectively) and were less than REMOTE ( $18 \pm 6\%$ ,  $P < 0.003$ ). However, in HYPER, %S improved at week 7 from  $9 \pm 8\%$  to  $18 \pm 5\%$  ( $P < 0.001$  versus week 1). In contrast, HYPO did not improve significantly ( $5 \pm 4\%$  to  $6 \pm 3\%$ ,  $P = \text{NS}$ ) and COMB tended to improve  $7 \pm 6\%$  to  $11 \pm 6\%$  ( $P = 0.06$ ).

**Conclusions**—HYPER has partially reversible dysfunction and represents predominantly viable myocardium. COMB shows borderline improvement and likely contains an admixture of viable and necrotic myocardium. HYPO shows little functional improvement at 7 weeks, presumably because of irreversible myocardial damage. (*Circulation*. 1999;99:744-750.)

**Key Words:** magnetic resonance imaging ■ reperfusion ■ contrast media

Prompt reperfusion salvages myocardium at risk after coronary artery occlusion.<sup>1,2</sup> Significant improvement in mortality and morbidity may be achieved even when reperfusion occurs up to 6 to 12 hours after acute myocardial infarction (MI).<sup>3</sup> However, protracted ischemia may produce an admixture of necrotic and viable myocardium. Although stunned viable myocardium differs structurally and metabolically from irreversibly injured myocardium, both may display similarly depressed mechanical function at rest early after MI.

## See p 727

Recently, a number of studies have investigated the potential value of T1-shortening contrast agents, combined with rapid MRI, in the characterization of regional myocardial perfusion, ischemia, and infarction with and without reperfusion.<sup>4-10</sup> Normal myocardium displays signal enhancement immediately after passage of the contrast bolus through the left ventricle (LV) because of the T1 shortening effect of the contrast material. Previously ischemic, reperfused myocardium has been shown to display 2 different types of contrast

“defects”: first-pass regions of reduced signal enhancement and regions with relatively increased signal intensity on delayed images.<sup>6,7</sup> The relationship between these 2 patterns and subsequent regional recovery of mechanical function has not been determined. In addition, most previous studies have used only delayed imaging, but it is now possible to image dynamically through the first-pass period. Thus, the goals of the present study were to combine first-pass and delayed image data to assess contrast abnormalities and to quantify the relationship between changes in regional mechanical function between 1 and 7 weeks after MI in regions with abnormal contrast patterns by use of myocardial tissue tagging.

## Methods

### Subject Population

Twenty-seven subjects, 10 normal (from medical history and age) control subjects who underwent contrast imaging only (4 men; mean age,  $37 \pm 6$  years) and 17 patients (14 men) with a mean age of  $53 \pm 12$  years were included. Patients were studied after a reperfused first MI. Average time from initial cardiac symptoms to initiation of reperfusion therapy was  $280 \pm 170$  minutes. Table 1 summarizes the

Received June 8, 1998; revision received October 16, 1998; accepted October 26, 1998.

From the Division of Cardiology, Department of Medicine, Allegheny General Hospital, Pittsburgh, Pa.

Correspondence to Walter J. Rogers, Jr, MS, Division of Cardiology, Allegheny General Hospital, 320 E North Ave, Pittsburgh, PA 15212.

© 1999 American Heart Association, Inc.

*Circulation* is available at <http://www.circulationaha.org>

TABLE 1. Patient Characteristics

Patient	Age, y	Sex	CPK, U/L	EF, %	Site	Time, d	Lytic	PTCA	HYPER	HYP0	COMB
1	33	M	5505	35	Ant	4	—	+	—	—	+
2	63	M	2838	30	Ant	10	—	+	+	—	+
3	45	F	3120	45	Ant	9	—	+	—	+	—
4	56	F	963	35	Ant	3	—	+	+	—	—
5	57	M	1894	45	Ant	4	—	+	+	—	+
6	45	M	4080	40	Ant	5	—	+	—	+	+
7	60	M	2385	25	Ant	6	—	+	+	—	—
8	44	M	2123	28	Ant	3	+	+	—	+	+
9	36	M	923	50	Ant	3	—	+	+	—	+
10	72	F	302	35	Ant	3	—	+	+	—	—
11	56	M	4428	45	Inf	4	—	+	+	—	+
12	48	F	1211	30	Ant	4	—	+	+	—	—
13	55	M	1401	40	Inf	3	—	+	+	—	+
14	38	M	3940	23	Ant	4	+	+	+	+	+
15	76	M	909	45	Ant	8	—	+	+	—	+
16	58	M	3540	45	Ant	3	—	+	+	—	—
17	54	M	3890	50	Inf	5	+	—	+	+	—

CPK indicates creatine phosphokinase; EF, initial ejection fraction; Site, location of LV ischemia; Ant, anterior; Inf, inferior; Time, days from infarction to MRI; Lytic, use of thrombolytic agent to restore coronary flow; and PTCA, use of PTCA to restore coronary flow.

clinical parameters associated with each patient. All patients had TIMI grade 3 flow in the infarct-related artery after therapy and before week 1 contrast MRI.

### Image Acquisition

The normal control group underwent first-pass and delayed contrast-enhanced imaging to establish normal values for contrast kinetics and regional signal variability. In patients, MRI was performed 1 ( $5 \pm 2$  days) and 7 ( $7 \pm 2$  weeks) weeks after MI. We used a Siemens 1.5-T clinical scanner with patients in the prone position using an elliptical surface receiver coil. Scout images in the coronal and parasagittal long axis were used to identify the LV short and long axes. End systole was timed on the basis of minimum cavity area from a rapid midlevel short-axis cine with a time of resistance of 40 ms and a matrix of  $64 \times 128$ .

Tagged short-axis cine-segmented k-space MRI allowed data to be gathered during breath-hold periods of 16 to 18 cardiac cycles. Contiguous 7-mm short-axis slices were acquired from the LV apex to base at weeks 1 and 7. Seven phase lines were acquired for every cardiac cycle. A  $280 \times 280$ -mm field of view was imaged, including 112 to 126 phase lines and 256 frequency lines. Two sets of perpendicularly oriented tags, with 7-mm interstripe spacing, were generated by use of binomial radiofrequency pulses immediately before image acquisition. Images were acquired at 5 points across the cardiac cycle, with interphase delay adjusted to ensure timing of an image at end systole.

To position the contrast image plane, tagged short-axis images at multiple levels were reviewed in cine format to locate the region of mechanical dysfunction in each patient. On the basis of this information, a tagged long-axis cine was acquired in the center of dysfunction in the short axis to verify dysfunction in the same plane that would be used for the contrast-enhanced images. Contrast-enhanced images were acquired at week 1 with 0.1 mmol/kg nonionic gadolinium (Gadoteridol, Bracco Diagnostics) as described by Atkinson et al.<sup>11</sup> A venous line was positioned in the antecubital vein, and a contrast bolus was injected by hand over 4 to 6 seconds. T1-weighted, inversion-prepared Turboflash images were then sequentially acquired at a single location immediately after contrast injection (repetition time=rr interval, matrix= $96 \times 128$ , echo time=2 ms, flip angle= $10^\circ$ , slice thickness=10 mm, and field of view=30 cm) in the center of the dysfunctional region. A sufficient

number of images were acquired before contrast arrival in the LV to allow magnetization to reach steady state. The delay from the  $180^\circ$  inversion pulse to image acquisition was adjusted to minimize steady-state myocardial signal. Thus, images were acquired in diastole. A complete image was acquired in 360 ms during each of 64 sequential cardiac cycles. A delayed set of 10 inversion recovery images was acquired in the same orientation  $7 \pm 2$  minutes after contrast administration.

### Image Analysis

First-pass and delayed contrast images were reviewed in cine format and used in combination to define 2 types of abnormal contrast pattern qualitatively. On the first-pass images, regions were classified by 2 experienced, blinded observers as either normal in intensity or hypointense. On the delayed images, regions were characterized as normal in intensity or hyperintense. Regions displaying first-pass hypoenhancement without delayed hyperenhancement were defined as HYP0. Regions displaying no first-pass HYP0 but delayed hyperenhancement were defined as HYPER. Regions displaying combined first-pass hypoenhancement and delayed hyperenhancement were defined as COMB. Normal-appearing regions remote from either functional or contrast abnormalities were defined as REMOTE.

Contrast images were reviewed by 2 blinded reviewers for determination of location and transmural extent of contrast patterns. Defects were defined as being limited to the endocardial half of the LV wall (ENDO), the epicardial half of the wall (EPI), or transmural (TRANS).

Matching between week 1 tagged short- and long-axis perfusion images was accomplished with a custom computer program. The 3-dimensional coordinates defining the tagged short-axis image plane locations were graphically superimposed on the long-axis contrast image that best represented HYP0 and HYPER in the first-pass and delayed postcontrast images, respectively (Figure 1). Intersections between contrast defects and short-axis tagged image locations were used to select the tagged short-axis image planes that would be used for analysis of segment shortening (%S). In addition, the circumferential location and transmural extent (EPI, ENDO, or TRANS) of the contrast abnormality were matched to the tagged images to assign %S loci to HYP0, HYPER, COMB, or REMOTE. The transmural and circumferential locations used to compute %S at

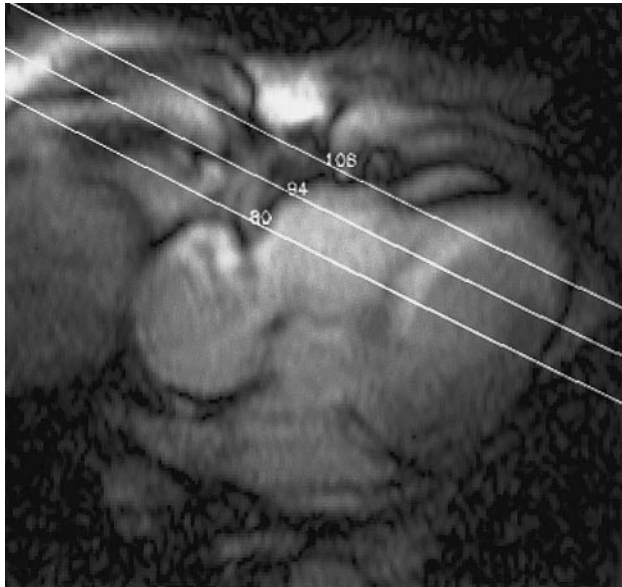


**Figure 1.** Contrast-enhanced MRI image acquired 9 minutes after gadolinium administration. Four-chamber orientation shows region of increased signal intensity (HYPER) within septum and apex. Of 7 acquired tagged short-axis image locations, 3 are displayed (white lines) intersecting HYPER contrast region.

week 1 were used for analysis of week 7 function. Slice level between weeks 1 and 7 tagged short-axis images was matched by use of internal landmarks such as papillary muscles, right ventricular insertion points, and absolute distance from the apex.

### Contrast Quantification

In patients, time-intensity curves, including initial and delayed time points, were calculated for regions of interest (ROIs) positioned within HYPO, HYPER, COMB, and REMOTE myocardium. Because of position-dependent changes in signal intensity resulting from the use of a surface receiver coil, curves were normalized in both patients and control subjects by dividing the absolute signal intensity by the value obtained in the same ROI before contrast arrival in the LV but after steady-state magnetization was reached. Normalized time-intensity curves were used to determine the signal intensity in HYPO (at peak first-pass REMOTE myocardial signal enhancement) and HYPER (in delayed images) relative to that in REMOTE in patients during the first-pass period and delayed contrast enhancement.

Signal intensity data in the control group were measured with 5 equally spaced circular ROIs (mean area, 0.4 cm<sup>2</sup>). Measurements before enhancement, at peak signal enhancement, and in delayed images were used to compute regional signal variability (expressed as the coefficient of variation) and the normal signal range (mean  $\pm$  2 SD). Visually selected HYPO and HYPER in patients were then quantitatively compared with the normal range.

### Mechanical Function Analysis

Regional myocardial percent circumferential %S from end diastole to mechanical end systole was calculated with the VIDA software package (University of Iowa) as previously described.<sup>12</sup> %S was measured at 3 transmural locations (epicardium, middle, and endocardium) at each circumferential location and for all locations by a trained observer (T.M.T.) with no knowledge of contrast imaging results. Results for %S at weeks 1 and 7 were compared in HYPO, COMB, HYPER, and REMOTE.

### Statistical Analysis

Results are expressed as mean  $\pm$  SD. Group differences in %S between regions and time points were tested by the independent-

samples *t* test or the nonparametric Mann-Whitney rank-sum test. Individual differences were tested by use of Fisher (least-significant-difference) posttest analysis. ANOVA with Fisher's posttest analysis was used to test differences between REMOTE, HYPER, and HYPO signal intensities during first-pass and delayed image acquisitions by analysis of time-intensity curves. Reproducibility between observers was tested by use of the  $\kappa$  statistic. The coefficient of variation was used to express the variability of relative postcontrast signal intensity within the LV in the normal control and patient groups.

## Results

### Contrast Kinetics

#### Normal Control Subjects

Normal myocardium displayed rapid, uniform first-pass signal enhancement and a lack of delayed regional hyperenhancement. The coefficients of variation for the 5 ROIs evenly distributed within the long-axis contrast enhanced images were 12.7% at peak enhancement and 15.2% on delayed images. The mean signal intensity relative to a reference ROI was  $1.02 \pm 0.1$ , resulting in a  $\pm 2$ -SD range of 0.82 to 1.22 at peak enhancement. On delayed images, the mean relative signal intensity was  $0.98 \pm 0.15$  of the reference ROI, resulting in a  $\pm 2$ -SD range of 0.68 to 1.28. These values were used to verify HYPO and HYPER in the patient group.

#### Patients

Contrast imaging in the 17 patients identified 5 HYPO, 13 HYPER, 10 COMB, and 17 REMOTE for a total of 28 regions. It was possible to have >1 abnormal contrast region in each patient. HYPO and HYPER were validated by comparison with quantitative data from the 10 normal control subjects. In regions visually identified as HYPO or COMB, 15 of 15 (100%) had relative signal intensity >2 SD below mean normal values on first-pass images. In regions identified as HYPER, 11 of 13 (85%) had relative signal intensity >2 SD above mean normal values on delayed images; the remaining 2 (15%) had signal intensity >1 SD above delayed mean normal. Of 10 regions defined as COMB, 6 (60%) had relative signal intensity on delayed imaging >2 SD above normal delayed values, 3 (30%) were >1 SD above normal, and 1 (10%) was <1 SD above the mean normal delayed value.

Figure 2 shows time-intensity curves for ROIs positioned in the LV blood pool, REMOTE, and HYPO regions for a sample patient during myocardial contrast transit. After a rapid increase in blood pool signal intensity, there is an early and persistent difference in myocardial signal intensity between HYPO and REMOTE. HYPO is seen as a subendocardial region of hypointense signal in the apical-septum in a first-pass, 4-chamber long-axis image of the same patient (Figure 3). In contrast, in HYPER (Figure 4), the early signal increase is similar between HYPER and REMOTE. However, the signal intensity in HYPER continues to increase, whereas REMOTE reaches a plateau. This produces hyperintense myocardium on the delayed postcontrast image shown in Figure 1.

#### Quantitative Analysis of First-Pass Signal Intensity in Patients

During the first pass of the contrast bolus, signal enhancement in HYPO was  $52 \pm 27\%$  of that seen in REMOTE

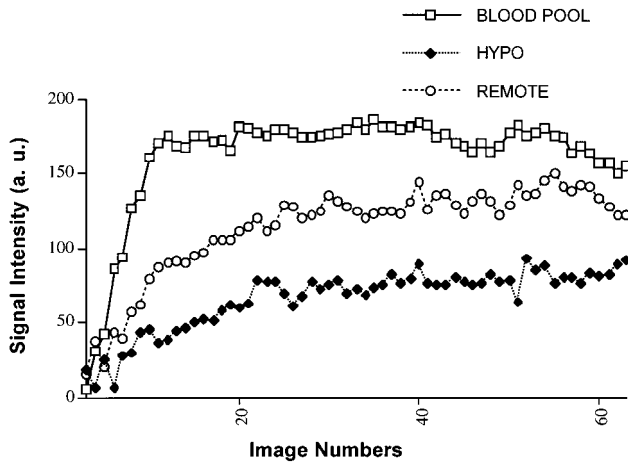


**Figure 2.** Time-intensity curves from LV blood pool (□), REMOTE (○), and HYPO (◆) regions. Curves derived from initial 63 successive images after contrast administration show persistent reduction in signal intensity vs REMOTE.

( $P < 0.0001$ ), whereas the signal intensity in HYPER was similar to REMOTE ( $91 \pm 31\%$ ). In delayed contrast imaging, HYPER increased to  $139 \pm 38\%$  of REMOTE ( $P < 0.003$ ). Signal enhancement in HYPO normalized in delayed images ( $80 \pm 38\%$  of REMOTE,  $P = \text{NS}$ ). COMB showed first-pass signal hypoenhancement ( $36 \pm 24\%$ ), which was different from both REMOTE and HYPER ( $P < 0.001$ ) but not from HYPO. Delayed-imaging hyperenhancement in COMB was  $159 \pm 68\%$  of remote ( $P < 0.01$ ). This was similar to HYPER and greater than observed in delayed HYPO ( $P < 0.04$ ). Table 2 displays the results of interobserver reproducibility in qualitatively identifying the type, location, and transmuralty of myocardial contrast patterns.



**Figure 3.** MRI first-pass contrast-enhanced image in 4-chamber long-axis orientation. Blood pool and myocardium in lateral wall show enhancement; septum and apex display region of hypo-enhancement.

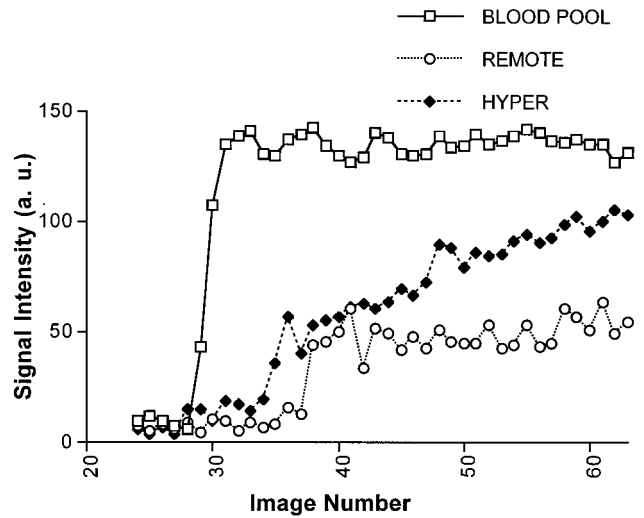


**Figure 4.** Time-intensity curves from regions in LV blood pool (□), REMOTE (○), and HYPER (◆) regions. Curves show that REMOTE reaches signal intensity plateau and HYPER continues to increase.

**Relationship Between Contrast Abnormalities and Mechanical Function Over Time**

Figure 5 compares 2 midlevel end-systolic short-axis tagged images of a patient displaying anteroseptal HYPER. Depressed myocardial deformation at week 1 is seen as a region of undeformed tag grid (arrow) in the anteroseptal region. The same portion of the LV displays noticeable improvement at week 7 (right) as indicated by a normal tag deformation pattern. Figure 6 displays %S data for HYPO, COMB, and HYPER regions at weeks 1 and 7. At week 1, %S was similar in HYPO, COMB, and HYPER at  $5 \pm 6\%$ ,  $7 \pm 6\%$ , and  $9 \pm 8\%$ , respectively. %S in these 3 groups was significantly less ( $P < 0.003$ ) than the  $18 \pm 6\%$  measured in REMOTE. By week 7, however, %S in HYPER had improved substantially to  $18 \pm 5\%$  ( $P < 0.001$  versus week 1), whereas the change in %S within HYPO to  $7 \pm 6\%$  was not significant. There was borderline improvement in %S in COMB from  $7 \pm 6\%$  to  $11 \pm 5\%$  ( $P = 0.06$ ). REMOTE %S increased to  $21 \pm 4\%$

**TABLE 2.  $\kappa$  Statistic for Interobserver Agreement**

Transmuralty	Location	First Pass	Delayed
ENDO	Septum	0.88	0.67
	Apex	0.67	0.69
	Lateral	1.00	1.00
	Inferior	1.00	1.00
EPI	Septum	*	0.50
	Apex	0.55	0.88
	Lateral	1.00	1.00
	Inferior	†	1.00

The  $\kappa$  statistic measures the agreement between the evaluation of 2 raters when both are rating the same object.  $\kappa = 1.0$  denotes perfect agreement;  $\kappa > 0.75$  denotes excellent reproducibility,  $0.4 \leq \kappa \leq 0.75$  denotes good reproducibility; and  $0 \leq \kappa < 0.4$  denotes marginal reproducibility.

\* $\kappa$  statistic could not be computed because the table was nonsymmetrical.

† $\kappa$  statistic could not be computed because 1 variable upon which measures of association are computed is a constant.

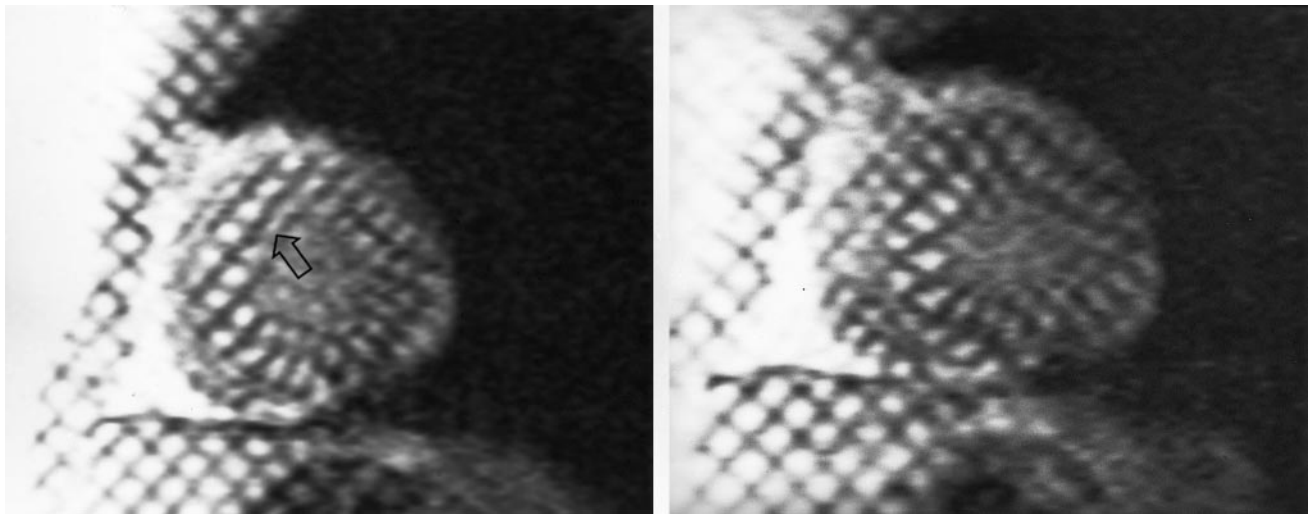


**Figure 5.** End-systolic midlevel short-axis tagged MRI images in patient at weeks 1 (left) and 7 (right) after myocardial reperfusion. Lack of myocardial deformation at week 1 is present in anteroseptal wall (arrow), which contained HYPER contrast pattern. Week 7 image shows return of normal tag deformation pattern in this region.

( $P=NS$  versus week 1). At week 7, HYPO, COMB, and HYPER displayed reduced %S compared with REMOTE ( $P<0.05$ ). HYPER displayed greater week 7 %S compared with COMB ( $18\pm 5\%$  versus  $11\pm 5\%$ ,  $P<0.005$ ) and HYPO ( $18\pm 5\%$  versus  $6\pm 3\%$ ,  $P<0.001$ ). At week 7, there was a trend toward greater %S in COMB versus HYPO ( $P=0.12$ ).

### Discussion

By combining information from first-pass and delayed MRI contrast-enhanced images with tissue tagging, we have shown

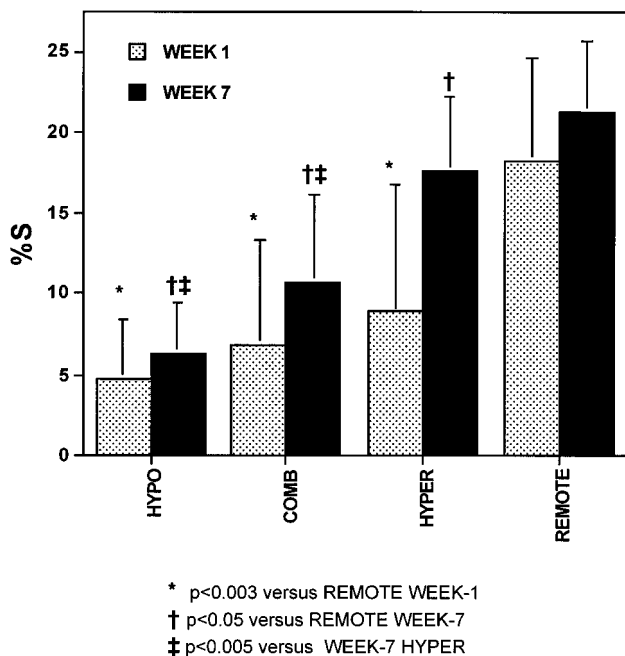


**Figure 6.** Change in %S between week 1- and 7-based contrast pattern. HYPO, COMB, and HYPER regions show reduced %S compared with REMOTE at week 1 ( $*P<0.003$ ). Function in these 3 contrast types was also reduced compared with REMOTE at week 7 ( $P<0.05$ ). At week 7, COMB and HYPO regions are reduced compared with HYPER ( $\ddagger P<0.005$ ).

that reperfused myocardial regions displaying a HYPER MRI contrast pattern show significant recovery of mechanical function at 7 weeks after MI. In contrast, HYPO does not show significant mechanical improvement, and there is a borderline improvement in COMB.

Our data and those from previous studies that used delayed imaging to identify HYPO (as defined in the present study) suggest that HYPO represents predominantly necrotic myocardium. Reduced signal intensity on first-pass MRI contrast images has been shown to be associated with reduced blood flow,<sup>4</sup> although this relationship may not be linear when higher doses of extravascular gadolinium-based MRI contrast agents are used.<sup>13</sup> In infarct regions, however, microvascular myocardial blood flow may not return to normal even after epicardial revascularization,<sup>14</sup> the so-called no-reflow phenomenon. In 2-day-old reperfused canine MI, Judd et al<sup>7</sup> reported a blunted and delayed increase in signal intensity in regions of infarcted myocardium. Hypointense regions correlated closely with regions delineated by thioflavin-S, a no-reflow marker. Regions of hypoenhancement have also been reported in patients with the use of a similar technique in healed infarcts after edema and other transient posts ischemic sequelae have likely resolved. Saeed et al<sup>10</sup> also demonstrated hypointense regions in a rat model after 3.5 hours of occlusion without reperfusion using gadodiamide and T1-weighted spin-echo images. Thus, the lack of normal, first-pass signal enhancement after a bolus injection of MRI contrast has been shown to identify myocardium with reduced blood flow and in the present study is associated with little late functional recovery.

A number of interrelated factors, including reduced regional blood flow,<sup>4,5,15</sup> increased capillary permeability,<sup>16</sup> and increased interstitial volume,<sup>17</sup> may produce HYPER within viable but previously ischemic myocardium. In the present study, HYPER differed in both contrast enhancement pattern and late myocardial function compared with HYPO, COMB, or REMOTE. The presence of regions with delayed hyper-enhancement by use of extravascular contrast agents has been

previously described.<sup>7,8</sup> Using an isolated rabbit heart preparation, Kim et al<sup>15</sup> quantified MRI contrast uptake and washout after reperfused MI. They concluded that hyperintense and hypointense contrast patterns are due primarily to alterations in wash-in/washout time constants that in turn result from differences in capillary density. Three different regions were analyzed: infarct center, infarct rim, and remote. These regions differed in extent and severity of ischemic damage and are roughly comparable to regions defined as HYPO, HYPER, and REMOTE in the present study. In the Kim et al<sup>15</sup> study, signal-to-intensity ratios compared with REMOTE during the early wash-in phase were  $40.4 \pm 2.1\%$  and  $84.9 \pm 3.6\%$  (mean  $\pm$  SEM) for infarct center and infarct rim, respectively. These were similar to our values of  $52 \pm 27\%$  and  $91 \pm 31\%$  for HYPO and HYPER, respectively. Kim et al<sup>15</sup> also reported infarct core and infarct rim signal intensity ratios of  $95.9 \pm 6.6\%$  and  $114.8 \pm 2.7\%$ , respectively, on delayed images. These are not dissimilar to our HYPO and HYPER values of  $80 \pm 38\%$  and  $139 \pm 38\%$ , respectively. We have shown that exclusively HYPER displays significant week 7 improvement and therefore must represent at least partially viable myocardium.

In a study evaluating MRI contrast patterns in patients after reperfused MI, Lima et al<sup>8</sup> found that there was a good correlation between fixed <sup>201</sup>Tl defect size and delayed contrast-enhanced MRI when both hyperintense and hypointense regions were combined but did not assess recovery of mechanical function. Fixed <sup>201</sup>Tl defects are often associated with nonviable myocardium. Thus, these data may seem to be at odds with the results of the present study. However, Lima et al<sup>6</sup> did not perform first-pass imaging. Furthermore, in the present study, all vessels had TIMI grade 3 flow before imaging, whereas the population studied by Lima et al included TIMI 0 to 3 flow. Incomplete reperfusion may account for such apparent reduced viability in HYPER. Another possibility may be that regions identified on stress-redistribution <sup>201</sup>Tl imaging as “fixed” may contain both viable and nonviable myocardium. Recently, Dilsizian et al<sup>18</sup> showed that <sup>201</sup>Tl reinjection identifies a significant volume of viable myocardium within “fixed” defects by stress-redistribution-reinjection <sup>201</sup>Tl scintigraphy. Judd et al<sup>7</sup> reported in a canine contrast MRI study that the hyperintense regions on delayed images were generally smaller than the risk region but larger (12%) than regions of necrosis as defined by triphenyltetrazolium chloride staining. This would indicate that at least part of the delayed hyperintense regions contain viable myocardium.

Yokota et al<sup>9</sup> used T1-weighted nonsegmented spin-echo imaging 5 to 10 minutes after Gd-DTPA administration in patients with nonreperfused myocardial infarction. They qualitatively compared contrast MRI results to peak creatine phosphokinase levels, wall motion, and coronary angiography and concluded that subendocardial or transmural hyperenhancement may reflect the existence of viable myocardium, whereas subendocardial hypoenhancement was associated with necrotic myocardium.

In the present study, there was a significant number (10 of 28) of abnormal regions that displayed both first-pass hypoenhancement and delayed hyperenhancement. It is likely

that this group contains an admixture of viable and nonviable myocardium. There was a trend for improvement from week 1 to 7 in COMB ( $P=0.12$ ) and for a difference in %S between COMB and HYPO in week 7 ( $P=0.06$ ).

### Study Limitations

%S measurements were repeated over time. This required matching of regions within the LV between weeks 1 and 7. Intrinsic cardiac landmarks were used to maintain registration as previously reported by Kramer et al<sup>19</sup> However, changes in LV shape or volume between imaging sessions could affect the precision of the match. Technical constraints limited MRI contrast imaging to a single image plane. Thus, care in positioning of the contrast plane in the center of the MI was essential. Given the limited spatial resolution of perfusion imaging, a conservative approach was assigning the transmural extent of contrast patterns as limited to EPI, the ENDO, or TRANS. There was a trend for greater week 7 %S in COMB versus HYPO ( $P=0.12$ ). Power analysis (independent-samples *t* test) indicated that analysis of an additional 12 subjects would result in a significant difference. Thus, the present study may be limited in detecting differences in %S between these 2 groups.

### Conclusions

Myocardium displaying hypoenhanced signal (HYPO) during first-pass transit, regardless of delayed contrast pattern, shows limited recovery of mechanical function by week 7 and is likely to be predominantly infarcted. In contrast, regions displaying hyperenhancement of delayed images in the absence of initial hypoenhancement show substantial functional late recovery and likely represent predominantly viable myocardium. Therefore, combining the information from first-pass and delayed contrast-enhanced MRI may predict late functional recovery in reperfused MI. Advances in MRI acquisition speed should permit imaging of all the LV during contrast first-pass and the delayed period, allowing clinically relevant application of the present study.

### References

1. Koren GT, Hasin Y, Appelbaum D, Luria MH, Gotsman MS. Prevention of myocardial damage in acute myocardial ischemia by early treatment with intravenous streptokinase. *N Engl J Med.* 1985;313:1384–1389.
2. Gruppo Italiano per lo Studio della Streptochinasi nell' Infarto Miocardico (GISSI). Effectiveness of intravenous thrombolytic treatment in acute myocardial infarction. *Lancet.* 1986;1:397–401.
3. Stone GW, Grines CL, Browne KF, Marco J, Rothbaum D, O'Keefe J, Hartzler GO, Overlie P, Donohue B, Chelliah N, Timmis GC, Vlietstra R, Strzelecki M, Puchrowicz-Ochocki S, O'Neill WW. Predictors of in-hospital and 6-month outcome after acute myocardial infarction in the reperfusion era: the Primary Angioplasty in Myocardial Infarction (PAMI) trial. *J Am Coll Cardiol.* 1995;25:370–377.
4. Wilke N, Simm C, Zhang J, Ellermann J, Ya X, Merkle H, Path G, Ludemann H, Bache RJ, Ugurbil K. Contrast-enhanced first-pass myocardial perfusion imaging: correlation between myocardial blood flow in dogs at rest and during hyperemia. *Magn Reson Med.* 1993;29:485–497.
5. Diesbourg LD, Prato FS, Wisenberg G, Drost DJ, Marshall TP, Carroll SE, O'Neill B. Quantification of myocardial blood flow and extracellular volumes using a bolus injection of Gd-DTPA: kinetic modeling in canine ischemic disease. *Magn Reson Med.* 1992;23:239–253.
6. Eichenberger AC, Schuiki E, Kochll VD, Amann FW, McKinnon GC, Schulthess GK. Ischemic heart disease: assessment with gadolinium-enhanced ultrafast MR imaging and dipyridamole-stress. *J Magn Reson Imaging.* 1994;4:425–431.

7. Judd RM, Lugo-Olivieri CH, Arai M, Kondo T, Croisille P, Lima JAC, Mohan V, Becker LC, Zerhouni EA. Physiological basis of myocardial contrast enhancement in fast magnetic resonance images of 2-day-old reperfused canine infarcts. *Circulation*. 1995;92:1902–1910.
8. Lima JAC, Judd RM, Bazille A, Schulman SP, Atalar E, Zerhouni EA. Regional heterogeneity of human myocardial infarcts demonstrated by contrast enhanced MRI: potential mechanisms. *Circulation*. 1995;92:1117–1125.
9. Yakota C, Nonogi H, Miyazaki S, Goto Y, Maeno M, Daikoku S, Itoh A, Haze K, Yamada N. Gadolinium-enhanced magnetic resonance imaging in acute myocardial infarction. *Am J Cardiol*. 1995;75:577–581.
10. Saeed M, Wendland M, Takehara Y, Masui Takayuki Higgins CB. Reperfusion and irreversible myocardial injury: identification with a nonionic MR imaging contrast medium. *Radiology*. 1992;182:675–683.
11. Atkinson DJ, Burstein D, Edelman RR. First-pass cardiac perfusion: evaluation with ultrafast MR imaging. *Radiology*. 1990;174:757–762.
12. Clark N, Reichek N, Bergey P, Hoffman EA, Brownson D, Palmon L, Axel L. Normal segmental myocardial function: assessment by magnetic resonance imaging using spatial modulation of magnetization. *Circulation*. 1991;84:67–74.
13. Burstein D, Taratuta E, Manning WJ. Factors in myocardial “perfusion” imaging with ultrafast MRI and Gd-DTPA administration. *Magn Reson Med*. 1991;20:299–305.
14. Kloner RA, Ganote CE, Jennings RB. The “no-reflow” phenomenon after temporary coronary occlusion in the dog. *J Clin Invest*. 1974;54:1496–1508.
15. Kim RJ, Chen R-L, Lima JAC, Judd RM. Myocardial Gd-DTPA kinetics determine MRI contrast enhancement and reflect the extent and severity of myocardial injury after acute reperfused infarction. *Circulation*. 1996;94:3318–3326.
16. Dauber IM, Van Benthuyzen KM, McMurtry IF, Wheeler GS, Lesnefsky EJ, Horwitz LD, Weil JV. Functional coronary microvascular injury evident as increased permeability due to brief ischemia and reperfusion. *Circ Res*. 1990;66:986–998.
17. Saeed M, Wendland MF, Masui T, Higgins CB. Reperfused myocardial infarctions on T1- and susceptibility-enhanced MRI: evidence for loss of compartmentalization of contrast media. *Magn Reson Med*. 1994;31:31–39.
18. Dilsizian V, Rocco TP, Freedman NMT, Leon MB, Bonow RO. Enhanced detection of ischemic but viable myocardium by the reinjection of thallium after stress-redistribution imaging. *N Engl J Med*. 1990;323:141–146.
19. Kramer CM, Rogers WJ, Theodobald TM, Power TP, Geskin G, Reichek N. Dissociation between changes in intramyocardial function and left ventricular volumes in the 8 weeks after first anterior myocardial infarction. *J Am Coll Cardiol*. 1997;30:1625–1632.